PEL-249

THE APPLICATION OF MATHEMATICAL MODELS FOR THE EVALUATION OF RADIOACTIVE TRACER TESTS CARRIED OUT IN SOUTH AFRICA

by

G.C. Snyman
and
S.W. Smith

PEL 249

ATOMIC ENERGY BOARD
Pelindaba
PRETORIA
Republic of South Africa

December, 1975

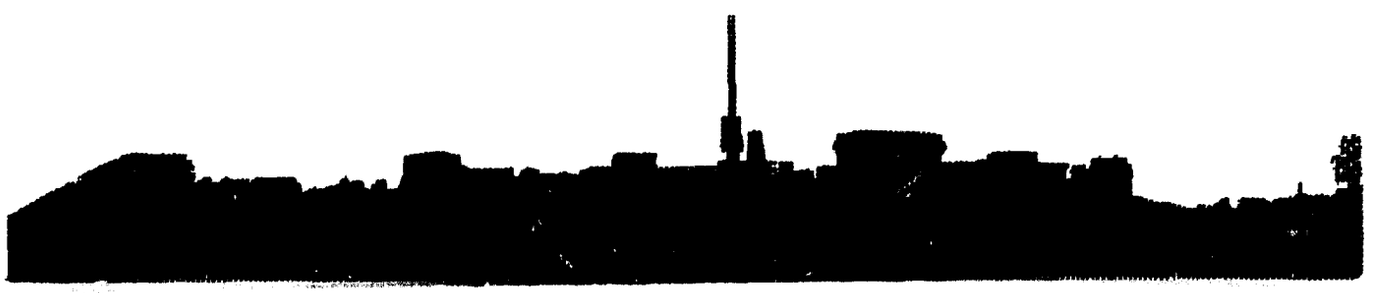

PEL-249-1

ATOMIC ENERGY BOARD

THE APPLICATION OF MATHEMATICAL MODELS FOR THE EVALUATION OF RADIOACTIVE TRACER TESTS CARRIED OUT IN SOUTH AFRICA

by

G.C. Snyman*
and
S.W. Smith*

*Isotopes and Radiation Division
POSTAL ADDRESS:
Private Bag X256,
PRETORIA
0001

PELINDABA
December, 1975

ISBN 0 86960 604 2

SUMMARY

The application of mathematical models to evaluate tracer experiments is illustrated by examples of tests done in a variety of industrial plants, using radioactive tracers. Two basic models, the axial mixing model and the perfectly mixed tank model, as well as various applicational techniques, are described.

It is concluded that many processes can be simulated to various degrees of accuracy by using the basic models, and that both quantitative and qualitative information can be obtained about the process.

SAMEVATTING

Die toepassing van wiskundige modelle om spoordertoetse te evalueer word geïllustreer deur voorbeelde van toetse wat in 'n verskeidenheid industriële aanlegte gedoen is met radioaktiewe spoorders. Twee basiese modelle, die aksiale vermengingsmodel en die ideale mengvatmodel, asook verskeie toepassingstegnieke, word beskryf.

Daar word tot die gevolgtrekking gekom dat baie prosesse deur middel van die basiese modelle tot verskillende grade van akkuraatheid gesimuleer kan word en dat kwantitatiewe sowel as kwalitatiewe inligting oor die proses ingewin kan word.

CONTENTS

1. INTRODUCTION

Radioisotopes have been used extensively in the past in South Africa as tracers to obtain mean residence times and mean residence-time distributions of process materials in various industrial process units [1, 2, 3]. The data obtained by such experiments often provide information about the process dynamics as well, so that it is desirable not only to report the response curves, but also to give an indication as to how well the system behaved, or which factor(s) possibly distorted the response or impaired the performance of the system. This type of information can be extracted from the data by means of the simulation of the measured response with the aid of theoretical models.

The advantages of the application of models can be summarised as follows:

(a) A better understanding of a particular process can be obtained. Models can also help to show up abnormal behaviour in systems.

(b) Models are usually fitted to the experimental data by means of least-squares computer programs. In this type of computation every data point contributes to the accuracy with which the process parameters are determined, and because this is a numerical technique, such accuracy is improved. Possible deviations in the parameters can easily be compared at the same time.

(c) Because models usually describe the response of a system to an impulse input, the saving on the amount of tracer material used for a particular test can be large. For example: compare the consumption of tracer used for the continuous injection technique of flow measurement, with the amounts required by the impulse technique.

(d) Many industrial processes do not operate at a steady state for long enough to allow a series of tests to be performed in single stages. Also the flow rates, etc. of a plant are usually not measured separately for each stage. A single pulse of tracer can be followed through all the stages, while the behaviour of single stages can still be derived with the aid of models. This usually results in a saving of tracer and labour.

(e) A good model can in many cases overcome crises such as a temporary loss of data through the failure of a detector, or a recorder going off scale for a short time. The model can still be fitted to the remaining data provided these data are reliable and the model is known to describe the system well. Under such circumstances the whole test can be saved with only a reduction in accuracy of the parameters.

(f) The evaluation of a system with recycle loops is practically impossible without a model. The measurement of the recycle rate in a process is in many cases possible only through a tracer test backed by a good model. This also applies to parallel flows in some systems.

This report describes models which were found most useful for a large variety of tracer tests on industrial plants. The application of the basic models and refinements of the models to actual radioactive tracer tests, are also described.

The models and their applications described here may not have been the best models for the given processes, but they served very well as first approximations, and helped to make useful deductions on the performance of the systems. A thorough look at the flow pattern in a particular process, and observations on the shape and delays of the measured impulse response, will usually suggest the starting point when building a model for a particular system.

2. BASIC THEORY OF MODELS

Any material-handling system can be schematically represented by Figure 1. The change caused by the system in the concentration versus time distribution of a tracer injected at the input is characteristic of the system, and the mathematical simulation of this change can disclose valuable information about the performance of the system. The process may be expressed mathematically as an input function, X(t), an output function, Y(t), and a transfer function, H(t). The simulation of data, collected as Y(t), involves the choice of a suitable transfer function, so that the choice of a relatively simple input function will simplify the treatment.

FIG 1 SCHEMATIC REPRESENTATION OF A MATERIAL HANDLING SYSTEM

2.1 The Delta Function

A very suitable input function, which can easily be simulated in practice, is the delta function $\delta(t)$. It is a discontinuous function and expresses mathematically a physical process of a sudden impulse, which is in practice achieved by the instantaneous release of the tracer. It may be expressed as

$$\delta(t) = 0,\ t \neq 0$$

$$\delta(t) = 1/\Delta t,\ t = 0,\ \Delta t \to 0$$

The delta function is further defined as having a unit area, i.e.:

$$\int_{-\infty}^{+\infty} \delta(t).dt = 1$$

The transfer function, H(t), is defined as the delta function response of the system, so that H(t) = Y(t) for a delta function input at t = 0.

2.2 The Convolution Integral

In many experiments it may be impossible or impractical to have a delta function input. If X(t) is known, the simulation of Y(t) is then achieved by considering X(t) to be composed of n pulses occurring at $t = T_1, T_2, \ldots\ldots, T_n$, each of duration ΔT and amplitude $X(T_i)$, and therefore of weight $X(T_i).\Delta T$. Because the transfer function is defined for an impulse at t = 0, and these pulses occur at $t = T_i$, the response of the system to one of the pulses may be given as:

$$Y_i(t) = H(t - T_i).X(T_i).\Delta T,$$

and the overall response:

$$Y(t) = \sum_{i=1}^{n} H(t - T_i).X(T_i).\Delta T \qquad \ldots (1)$$

Let $n \to \infty$, $\Delta T \to 0$

$$Y(t) = \int_0^t H(t - T).X(T).dT \qquad \ldots (2)$$

The upper limit of the integral is chosen at t, because X(T) cannot contribute to Y(t) if T > t.

Equation (2) is known as the convolution integral.

2.3 The Laplace Transform

In the derivation of the theoretical output function, differential equations are often encountered. These can be solved with relative ease by using the Laplace transform. The transform, f(s), of a function, f(t), is defined as:

$$L[f(t)] = f(s) = \int_0^\infty f(t).e^{-st}.dt,$$

where s is a complex variable.

Applied to equation (2),

$$Y(s) = H(s).X(s) \qquad \ldots (3)$$

The simple form of the latter equation has resulted in wide application of the Laplace transform in the field of tracer experiments.

The inverse transform of f(s) is:

$$f(t) = (1/2\pi i) \int_{a-i\infty}^{a+i\infty} e^{st}.f(s).ds$$

The inverse transformation of Laplace functions is often found to be the most tedious part of the analyses, mainly because of the nature of the integral. Inverse transforms of many functions are, however, readily available in the literature [4], and if the solution cannot be found there, numerical inversion methods [5, 6], though not so accurate, can be applied with success.

Even the most complex output function is basically of the form of equation (3). The convolution integral can therefore often be applied, either numerically or analytically, to obtain the inverse transform. The obvious disadvantage of this method is that the inverse transforms of both the functions forming the product must be known beforehand.

3. AXIAL MIXING MODEL

This model has been described in detail by several authors [7, 8, 9]. The model treats turbulent dispersion as mathematically analogous to molecular diffusion. In the one-dimensional case (along the main axes) the dispersion in a stationary medium may be described by the classical diffusion equation

$$E.\frac{\partial^2 C}{\partial x^2} = \frac{\partial C}{\partial t} \qquad \ldots (4)$$

The solution of equation (4) for a delta function input at x = 0 and t = 0 can be shown to be

$$C(x,t) = \frac{1}{\sqrt{4\pi Et}}.\exp(-x^2/4Et) \qquad \ldots (5)$$

where C(x, t) = concentration of tracer at time t in position x

E = dispersion coefficient.

Note that equation (5) is symmetrical about the origin x = 0. We did not have occasion to apply equation (5), but it is possible to visualize a number of situations where it could be used, e.g. for batch mixing in a circular drum with the main axis horizontal.

The measurement of flow in a pipe is a much more common problem. The medium is moving in one direction with a mean velocity u. The differential equation then becomes

$$E.\frac{\partial^2 C}{\partial x^2} = u.\frac{\partial C}{\partial x} + \frac{\partial C}{\partial t} \qquad \ldots (6)$$

Consider the problem where a unit planar pulse is injected at x = 0 and t = 0, and a detector is placed some distance x downstream to record the passage of the tracer. The solution of (6) then becomes

$$C(x, t) = \frac{1}{\sqrt{4\pi Et}}.\exp[-(x - ut)^2/4Et] \qquad \ldots (7)$$

Equation (7) is not symmetrical with time at the measuring point because it allows for dispersion while the pulse passes the measuring point. Equation (7) is very useful to fit to tracer problems where the tracer is injected at one point and the passage of the pulse is recorded some distance downstream of the injection point.

3.1 Application of Equation (7)

In order to determine the efficiency of the ventilation fan of the Kinross Gold Mine [10], it was necessary to measure the air flow rates in the inlet and outlet shafts. Figure 2 illustrates the problem. Both shafts were seven metres in diameter. Shaft number 1A was divided into two ducts by a partitioning wall. About two-thirds of the area was used as the stale-air outlet duct, and the remaining area was used in parallel with the number 1 shaft for fresh-air downflow. The available test length was about 800 metres in each case. It was not possible to install a second detector between the injection points and the measuring points, as indicated in Figure 2.

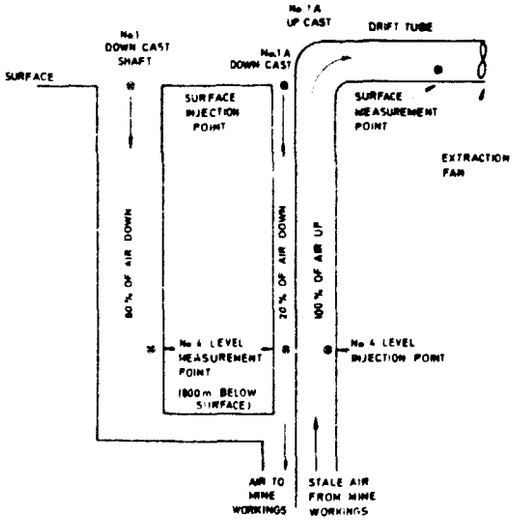

FIG 2 SCHEMATIC DIAGRAM OF SHAFTS USED FOR VENTILATION OF THE MINE

The axial mixing model described above required a planar injection of tracer. This was not possible, but from the work of several authors [11, 12, 13] it was estimated that the errors would be small if it was assumed that the point-injected tracer would mix radially over a relatively short distance. The two down-flowing airstreams were measured individually with one curie ^{85}Kr pulses, and the outlet airstream was measured with a 2 curie ^{85}Kr pulse. Beta-radiation detectors were used and the detector pulses were stored on magnetic tape.

We have taken this opportunity to compare the pulse-velocity technique with the total-count technique [14]. The total-count technique will not be described here, but it can be remarked that several days of preparation were required to measure the efficiency of the detectors as a function of pressure and humidity.

The pulse-velocity measurements required only three hours to perform.

Figure 3 shows the least-squares fit of the model described by equation (7) to the measured time-concentration curve. The mean velocities of the air flow in all three ducts were obtained, and the mass flow rate of air was calculated from measurements of a cross-sectional area of the shafts and the pressure and humidity readings. Table 1 summarizes the results and compares the results obtained using the two techniques. The agreement between upflow and downflow rates was better than 4 %.

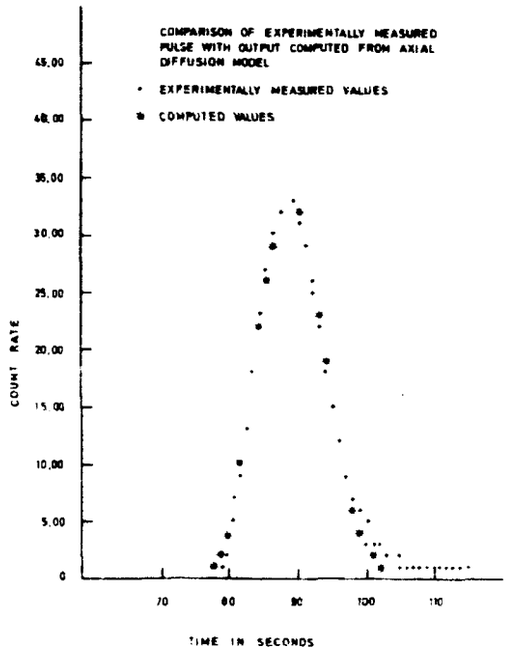

FIG 3 No.1A DOWNCAST SHAFT PULSE

TABLE I
COMPARISON OF PULSE-VELOCITY METHOD AND TOTAL-COUNT METHOD OF AIR FLOW IN MINE SHAFTS.

Shaft	Total-count method Flow rate (kg/sec)	Pulse-velocity method Flow rate (kg/sec)
1A up	468	466
1A down	115	119
1 down	349	368

3.2 Single Pulse with Multiple Detectors

As mentioned above, the weakness of the method described in the previous section lies in the injection of a planar pulse or the uncertainty on the radial mixing if this condition was not met. This weakness is overcome by using two detectors. The first detector is placed sufficiently downstream to ensure good radial mixing. The second detector is placed at a convenient distance further downstream. The mean-velocity measurement is done between the two detectors. The condition of good radial mixing is met at the first detector, but the input

pulse is not a delta function but a time-distributed pulse which is measured with the first detector. The transfer function between the first and second measuring point is derived as follows: (Refer to sections 2.2 and 3.4)

$C_1(x_1,s) = H_1(s).\,Q(s)$
$C_2(x_2,s) = H_2(s).\,Q(s)$

where $C_1(x_1,s)$ = Laplace transform of the measured pulse in x_1
$C_2(x_2,s)$ = Laplace transform of the measured pulse in x_2
$H_1(s)$ = Laplace transform of the delta function response over the first section (up to x_1)
$H_2(s)$ = Same as above up to x_2
$Q(s)$ = Laplace transform of the injected pulse at $x = 0$, $t = 0$.

To obtain the transfer function between the two measuring points,

$$C_2(x_2,s) = \frac{H_2(s)}{H_1(s)}.\,C_1(x_1,s) = H_3(s).C_1(x_1,s)$$

because of the common injected pulse Q(s).
Thus the transfer function is

$$H_3(t) = L^{-1}[H_3(s)] = L^{-1}\left[\frac{H_2(s)}{H_1(s)}\right]$$

$$= \frac{(x_2-x_1)}{\sqrt{4\pi Et^3}}.\exp[-(x_2-x_1-ut)^2/4Et] \qquad \ldots (8)$$

If the input pulse $C_1(x_1,t)$ at x_1 and the output pulse $C_2(x_2,t)$ at x_2 were measured with the two detectors, the input pulse can be convoluted onto the output pulse with $H_3(t)$:

$$C_2(x_2,t) = \int_0^t H_3(t-\tau).C_1(x_1,T).dT \qquad \ldots (9)$$

where $H_3(t-T)$ has the form of equation (8). Thus, by combining the convolution with a least-squares fit and varying the parameters u and E in $H_3(t)$, equation (9) is fitted to the experimental values of $C_1(x_1,t)$ and $C_2(x_2,t)$.

In some cases, particularly at low Reynolds numbers, the boundary layer of air along the pipe walls may contain an appreciable fraction of the tracer material. The result is a long tail on the measured time-concentration curves. Under these conditions the above model fails to describe the dispersion satisfactorily. For such skewed pulses, we have successfully assumed a transfer function in the form of a gamma fuction, e.g.,

$$H(t) = A.t^B.\exp(-Ct)$$

$$\text{or } H(t) = A.(t+\tau)^B.\exp[-C(t+\tau)] \qquad \ldots (10)$$

Convolution with equation (10) and the parameters A, B, C and τ, allows one to obtain a value of the average time $\bar{t}$ that an assumed delta-function input takes between the measuring points.

3.3 Application of Equation (9) to Gas Flow in Pipelines

The two-detector technique described in the previous section was used to do accurate volumetric flow-rate measurements in the gas mains of GASKOR [15]. Flow rates in the range 5 000 to 60 000 m^3/h at STP in pipelines with diameters of 150 to 350 mm were injected into the pipelines at convenient points. The first detector was mounted about 100 metres downstream on the outside of the pipe and the second detector a further 100 to 300 metres downstream. The outputs of the two detectors and the timing signals were recorded on magnetic tape. These recorded data were read back into the computer for analysis. Each measurement took only a few minutes to do. An added advantage was the fact that only a single access hole (for injection of the tracer) in the pipeline was required for a test.

Figure 4 is a typical example of the input pulse convoluted onto the measured output pulse using equation (9). The mean velocity and dispersion coefficient of the tracer in the gas stream was found by the least-squares method.

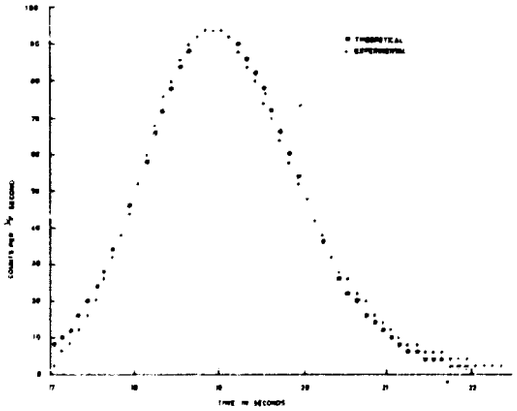

FIG 4. CONVOLUTED INPUT FITTED TO MEASURED RESPONSE

Unfortunately the only alternative gas-flow measurements available for comparison were accurate to within only one per cent. It is estimated that the results obtained with this method were accurate to within less than 0,2 %.

3.4 Application of Equation (9) to Flow of Gas in a Catalytic Cracker Reactor

The uneven distribution of temperature in a catalytic cracker reactor at the NATREF petroleum refinery indicated malfunctioning of the system [16]. Maldistribution of reactants in the catalyst bed was suspected. Since shutting down the system for an

inspection would have resulted in a substantial loss in production, the refinery wanted a second opinion on the possible cause of the uneven temperature distribution.

The refinery had a second reactor of similar design which was functioning well. Figure 5 shows a schematic diagram of the two reactors. The inputs (tops), outputs, and quench inputs (distributors) of the reactors were designed to ensure a very uniform flow of gas over the cross-sectional area of the catalyst bed (planar injection).

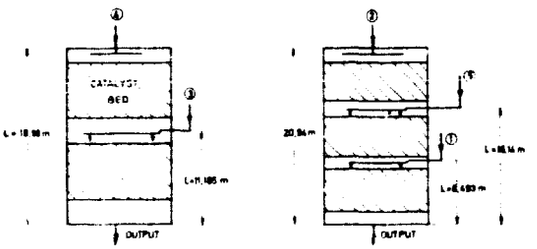

H.D.C. REACTOR D.H.C. REACTOR

FIG.5 SCHEMATIC DIAGRAM OF HYDROCRACKER REACTORS

We used the good reactor to test the theoretical model and to compare its response to that of the malfunctioning reactor.

Pulses of the tracer gas argon-41 were injected into the input points 1 to 5 indicated in Figure 5. The first detector was installed on the input gas line as near as possible to the distributor under test. The second detector was installed on the output line as near as possible to the bottom of the catalyst bed. Both the input and output pulses were recorded for each section under test. Equation (9) with transfer function (8) was used to convolute the recorded input pulses. Figure 6 shows how well this model fitted the response of the good reactor. Figure 7 shows that the output pulse of the malfunctioning reactor had a much longer tail than predicted by the model. This long tail indicated a stagnant volume in the catalyst bed and explained the uneven temperature distribution of the catalyst bed.

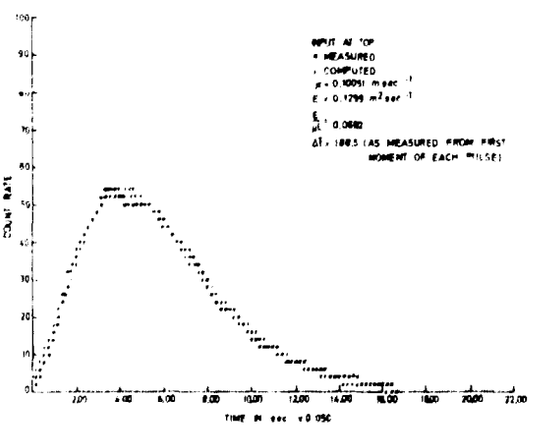

FIG.6 FIT OF COMPUTED OUTPUT ON MEASURED OUTPUT B.O.C. PULSE N° 4

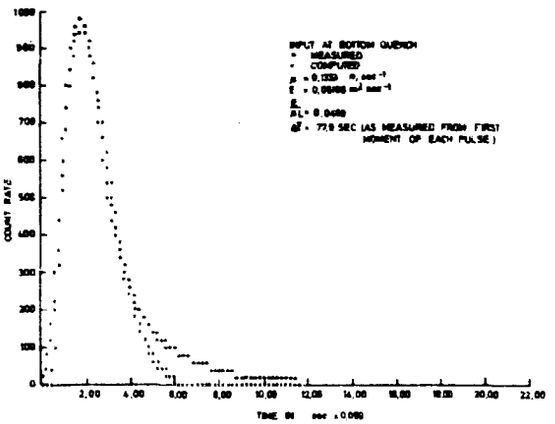

FIG.7 FIT OF COMPUTED OUTPUT ON MEASURED OUTPUT D.H.C. PULSE N° 1

This application shows that the model was of considerable help in deciding whether the response of the reactor was normal or abnormal.

3.5 Application of the Axial Mixing Model to a Sugar Crystallizer

The continuous crystallizer plant for massecuite at the Empangeni Mill of Huletts Sugar Limited consists of a number of vessels in series [17]. Figure 8 shows a schematic diagram. The contents of vessel number 6 undergo a circular stirring motion while all the other vessels have a reciprocating rocker type of stirrer. It was necessary to compare the behaviour of the two types of crystallizers in order to assess the desirability of converting the entire system to circular stirrers.

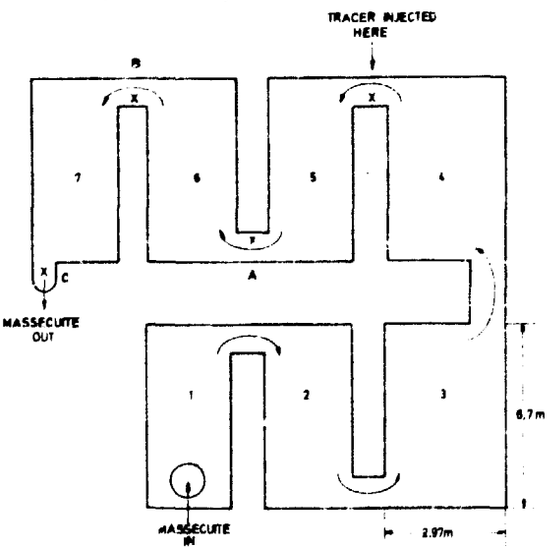

FIG.8 DIAGRAM OF THE C-CRYSTALLIZER INSTALLATION WITH DETECTORS AND SAMPLING POINTS AT POSITIONS A, B AND C

In continuous crystallizers it would be desirable to obtain, as nearly as possible, an ideal plug-flow condition in the axial direction with complete mixing in the radial direction of the vessel.

It was decided to carry out the test with a single pulse of tracer on the last three vessels of the

installation. Thus the output response curves of each of the three vessels could be used to compare the behaviour of each of the vessels with the other under the same conditions of massecuite flow.

A single pulse of 10 mCi of iodine-131 was used as a tracer. The tracer was obtained in the form of 3 ml of aqueous solution. This small amount of tracer was thoroughly mixed into one litre of massecuite to ensure that the tracer would correctly represent the highly viscous massecuite.

The tracer was injected with compressed air into the crossover gutter leading into vessel number 5. For the purpose of the analyses, this injection was assumed to be a delta-function input.

A lead-shielded scintillation detector with a collimator was mounted at the outlet of each of the three vessels. The count rates were recorded on three scalers and printed at regular time intervals. The recorded output response curves of vessels 5 to 7 are given in Figures 9 to 11.

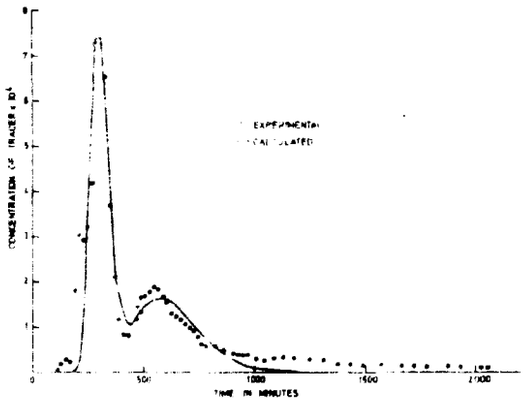

FIG 9 TWO PARAMETER DISPERSED PLUG FLOW MODEL APPLIED TO RESPONSE OF TANK 5

Vessel number 5 had a double-peak response, indicating parallel flow in two or more channels. The output of vessel number 6 was much smoother, indicating a single flow channel. Vessel number 7 had a double-peak response similar to that of vessel number 6.

3.5.1 EVALUATION OF THE RESULTS

The output of vessel number 5 could be described as the sum of two single dispersed pulses.

$C_1(x_1,t) = Q_a.C_a(x_1,t) + Q_b.C_b(x_1,t)$, where Q_a and Q_b amount of tracer in each channel, and $C_a(x_1,t)$ and $C_b(x_1,t)$ were of the form of equation (7). Thus two velocity and two dispersion coefficients and the split in flow rate could be found by the least-squares fit. Figure 9 shows the fitted response curve.

Vessel number 6 had a single flow channel. The measured output of vessel 5 was taken as the input of vessel 6, and this was convoluted with the measured output of vessel 6, using the transfer-function equation (3). The convoluted output is compared with the measured output in Figure 10.

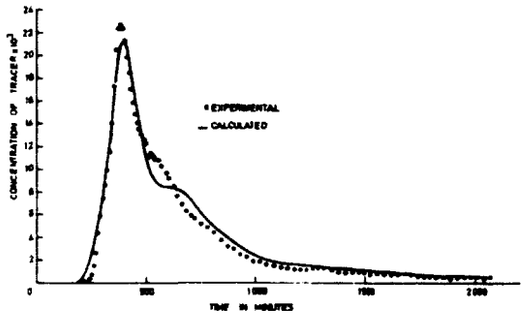

FIG 10 DISPERSED PLUG FLOW MODEL APPLIED TO RESPONSE OF TANK 6

The convolution technique was again applied for vessel number 7. The measured output of vessel number 6 was convoluted with the measured output, but the transfer function in this case was taken as a fraction of dispersed flow plus a fraction of plug flow:

$$C_3(x_3,t) = Q_a.C_a(x_3,t) + Q_b.C_2(x_2,t_b)$$

where $t_b = t - \dfrac{x_3 - x_2}{u_b}$

$C_a(x_3,t_a)$ was in the form of equation (9).

Figure 11 shows how this combination model fitted the output of vessel 7. From a knowledge of the total flow rate Q in the system of vessels, it was possible to calculate the dead volumes in each vessel. Vessel number 5 had no dead volume. Vessel number 6 had 70 % dead volume, and vessel number 7 had 43 % dead volume.

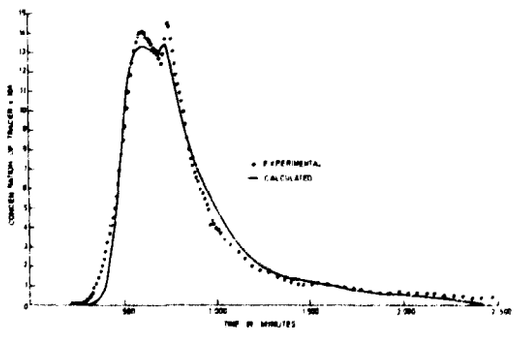

FIG 11 DISPERSED PLUG FLOW AND PLUG FLOW MODEL APPLIED TO RESPONSE OF TANK 7

It was concluded that the circular stirrer in vessel 6 resulted in a single channel flow through the middle of the vessel, with a large volume near the wall being wasted because the massecuite there had too high a viscosity. The small active volume of vessel 7 was

attributed to the increased viscosity of the massecuite in that vessel which solidified in the poorly agitated zones of the vessel.

4. PERFECTLY MIXED TANKS IN SERIES

Because of its adaptability to a large variety of applications, the perfectly mixed tank model is probably the best-known process simulator. Intricate flow patterns can be analysed with relative ease by the application of a combination of perfectly mixed tanks. The usefulness of the model will be illustrated in the following discussion.

Consider a string of perfectly mixed tanks of equal volume V', in series, through which passes a constant flow rate, Q. (Figure 12). Let $C_i(t)$ be the concentration in the i-th tank at time $t > 0$, resulting from a delta-function tracer injection at $t = 0$. According to the concept of perfect mixing, $C_i(t)$ is also the response function of the tank. A material balance on the i-th tank is:

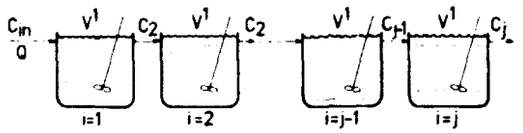

FIG 12 PERFECTLY MIXED TANKS IN SERIES

$$V'(dC_i(t)/dt) + Q.C_i(t) = Q.C_{i-1}(t) \qquad \ldots (11)$$

The solution of this equation is subject to two conditions set by the choice of a delta-function input. First, at $t = 0$, with no tracer present, $C_i(t) = 0$. This implies that

$$L[dC_i(t)/dt] = s.C_i(s)$$

Secondly, with tracer present at $t = 0$, the amount of tracer injected at $t = 0$ can be related to the mean concentration of tracer C_o when uniformly distributed in j tanks, as follows:

$$C_{in}(t).Q.\Delta t = C_o.V, \; t = 0, \qquad \ldots (12)$$

where V = total volume of j tanks = jV'
and $C_{in}(t)$ = initial concentration of tracer.

The Laplace transform of equation (11) is

$$V'.C_i(s).s + Q.C_i(s) = Q.C_{i-1}(s)$$

Solving for the j-th tank,

$$\begin{aligned} C_j(s) &= C_{j-1}(s)/[s(V'/Q) + 1] \\ &= C_{j-2}(s)/[s(V'/Q) + 1]^2 \\ &\vdots \\ &= C_{in}(s)/[s(V'/Q) + 1]^j \end{aligned}$$

But, from equation (12),

$$C_{in}(s) = C_o(V/Q)\int_0^\infty \delta(t).e^{-st}.dt$$

which can be proved to be

$C_{in}(s) = C_o(V/Q)$, so that

$$C_j(s) = C_o(V/Q)/[s(V/jQ) + 1]^j$$

The inverse transform is

$$C_j(t) = C_o(V/Q).(jQ/V)^j.(1/(j-1)!\,).t^{j-1}.\exp(-jQt/V)$$

The mean residence time of material in any vessel can be found from the first moment of area about $t = 0$, i.e.

$$\bar{t} = \frac{\int_0^\infty t.C(t).dt}{\int_0^\infty C(t).dt} \qquad \ldots (14)$$

Applied to equation (13),

$$\bar{t} = V/Q = jV'/Q \qquad \ldots (15)$$

Substituting $\bar{t} = V/Q$ in equation (13),

$$C_j(t) = C_o(j^j/(j-1)!\,).(t/\bar{t})^{j-1}.\exp(-jt/\bar{t}) \qquad \ldots (16)$$

The transfer function can be found by dividing $C_j(t)$ by the area, which is found by

$$\int_0^\infty C_j(t).dt = C_o.\bar{t} \qquad \ldots (17)$$

This can be verified by rearranging equation (12) as follows:

$$C_{in}(t).\Delta t = C_o(V/Q) = C_o.\bar{t}$$

The expression on the left is the area under the input pulse, which should equal that of the output distribution.

Finally, the transfer function is

$$\begin{aligned} H(t) &= C_j(t)/(C_o.\bar{t}) \\ &= (j^j/(j-1)!\,).(t^{j-1}/\bar{t}^j).\exp(-jt/\bar{t}) \qquad \ldots (18) \end{aligned}$$

and $H(s) = 1/[s(\bar{t}/j) + 1]^j \qquad \ldots (19)$

Because of the normalizing properties (unit area) of equation (18), data is often reported in this form, for ease of comparison between different curves.

5. APPLICATIONS OF THE TANKS-IN-SERIES MODEL

The operational principles of industrial equipment often bear a resemblance to the perfectly mixed tank. Perfect mixing is, however, rarely attained in practice. Poor mixing results in the formation of stagnant volumes, dead volumes and multiple mixing zones in the vessel, so that the operating parameters of the unit can be determined only by a tracer test. Although several 'real' mixed tank models are proposed in the literature [7, 18], practice has shown that each case has to be treated according to its own merits.

Examples of tracer experiments on industrial equipment with varying degrees of mixing will now be discussed.

5.1 The Basic Model

5.1.1 TANKS IN SERIES

Examples of the direct application of the tanks-in-series model can be found in the leaching vessels of gold recovery plants. The contact time of solids and cyanide is of prime importance because it affects the recovery of gold. The leaching is done in Brown tanks or Pachucas, which are designed to provide the maximum mixing efficiency to the contents by means of compressed air. A schematic representation of a typical plant is shown in Figure 13.

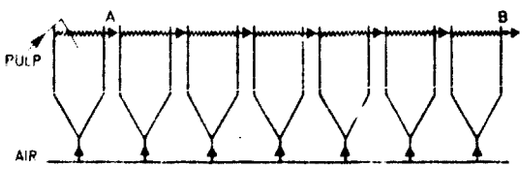

FIG 13 SCHEMATIC ARRANGEMENT OF TANKS AND MEASURING POINTS

An experiment done at the Libanon Gold Mine required that both the liquid and solids be traced [19]. The liquid tracer was prepared by irradiating tetrachlorogoldacid ($H(AuCl_2).3H_2O$) in the reactor, thus producing about 100 mCi of ^{198}Au, and dissolving the activated compound in a cyanide solution just prior to the injection. The choice of a gold/cyanide complex ensured that the tracer would stay in solution in the plant conditions. The isotopes of longer half-life (^{59}Fe, ^{46}Sc and ^{60}Co) of reactor-activated gold ore were used as the solids tracer. After allowing the shorter-lived isotopes to decay for two weeks, the remaining activity was about 45 mCi. By using the ore itself as tracer, the tracer response was certain to be representative of the solids' behaviour.

The tracers were injected simultaneously and the response of the tanks monitored by sampling the output at regular time intervals. After the solids and liquid in the samples had been separated by conventional methods, the activity in each of the samples was determined by counting on a 200 x 100 mm sodium iodide detector in a low-background castle. The resulting data were corrected for background and decay.

The mixing characteristics of the system could then be evaluated by fitting equation (16), with $j = 1$ and $j = 7$, to the data by means of a digital computer [20]. In this way, the parameters in the equation, viz. $\bar{t}$ and C_o, were solved to within an accuracy of 1 %. The fits are shown in Figures 14 and 15, which show that the tanks-in-series model successfully predicted the response.

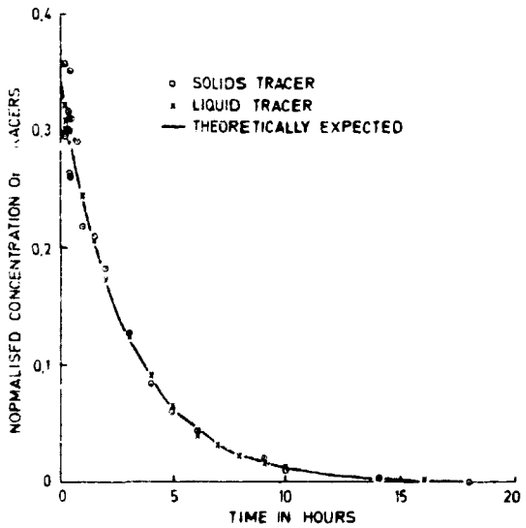

FIG 14 NORMALISED RESPONSE CURVES OF SOLIDS AND LIQUID AT MEASURING POINT A ON THE FIRST TANK

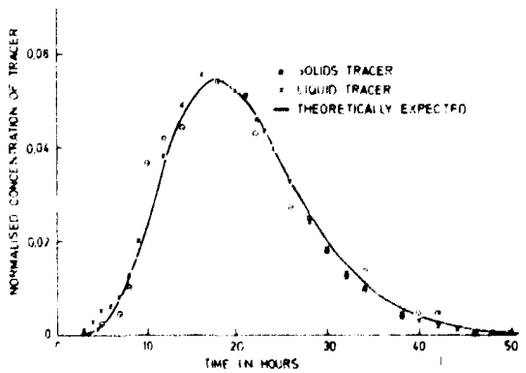

FIG 15 NORMALISED RESPONSE CURVES OF SOLIDS AND LIQUID AT MEASURING POINT B ON THE SEVENTH TANK

The mean residence time of the seven tanks was found to be 20,09 h for the liquid and 20,44 h for the solids. By calculating the mean residence time from equation (15), using the physical volumes of the tanks and the average flow rate during the experiment, it was found to be 20,66 h. This indicated that a small amount of dead volume had formed in the tanks. Dead volume is defined as the volume of material not partaking in the mixing, and may be calculated as

$$V_{dead} = V_{total} - V_{live}$$

= Physical Volume – (Measured $\bar{t}$ x Measured Flow Rate)

A dead volume of about 2 % was determined in this way. This may have been due to the volume of air present in the tanks, seeing that the physical volume had not been corrected in this regard.

A small amount of short-circuiting was also detected in the system. It is seen in the liquid response of Figure 15 as the delay in the leading part of the theoretical curve. This also affected the mean residence time.

It should be mentioned at this stage that the mean residence time could also have been calculated by taking moments of area (equation (14) in numerical form). The disadvantage of this technique is that large errors may arise from the less accurate data (due to counting statistics) of the trailing part of the response. These errors are amplified when multiplied by the larger moments of the trailing part. The modelling technique, on the other hand, treats all data as having the same weight, and is also less affected by scatter and scarcity of data.

5.1.2 COMPLEX MODELLING

The modelling of a more complicated material-handling system will now be discussed as a typical example of the adaptability of the perfectly mixed tank model.

An experiment similar to that described in 5.1.1 was done on the gold leaching plant of the Vaal Reefs North Gold Mine [21], shown schematically in Figure 16. Samples were taken at points A and B to determine the mean residence times of the first tank and the complete system. For the purposes of modelling, each tank was considered to be a perfectly mixed tank, and the volumes of pipes and ducts between tanks were considered to be negligible compared to the volumes of the tanks. The plant was divided into three sections (as shown in Figure 16), the transfer functions of the sections derived, and then combined to yield the overall response function.

The first section consisted of two tanks in series. The overflows of the tanks were returned to the input by means of a feed pump. Although the dimensions of the tanks were the same, the material level in the tanks,

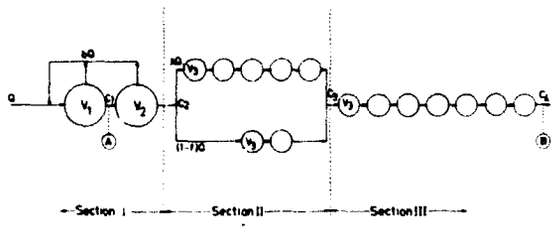

FIG 16 COMPLEX ARRANGEMENT OF LEACHING PACHUCAS

and consequently the recycle flow, varied during the experiment, so that the tanks had to be modelled as though they had different volumes, and the recycle fraction treated as an unknown parameter.

Let V_1 and V_2 be the volumes of the tanks, and b the fraction of the flow rate, Q, that is recycled from the second to the first tank. The recycle on the first tank is considered to be part of the mixing of the tank and is not included in the analysis. If $C_1(t)$ and $C_2(t)$ are the concentrations of tracer at the output of V_1 and V_2 respectively, and $C_{in}(t)$ the amplitude of a delta-function input at t = 0, material balances can be set up, viz.:

$$\bar{t}_1.C_1(s).s + C_1(s) = C_{in}(s)/(1+b) + C_2(s).b/(1+b) \quad \ldots (20)$$

and $$\bar{t}_2.C_2(s).s + C_2(s) = C_1(s) \quad \ldots (21)$$

where $\bar{t}_1$ and $\bar{t}_2$ are the mean residence times related to the actual flow rate, Q.(1+b), i.e.:

$$\bar{t}_1 = V_1/[Q.(1+b)]$$

$$\bar{t}_2 = V_2/[Q.(1+b)]$$

From equations (20) and (21) it can be shown that:

$$C_1(s) = \frac{C_{in}(s).(\bar{t}_2.s + 1)}{(\bar{t}_1.\bar{t}_2)(1+b)(s+P)(s+R)}$$

$$= C_{in}(s).H_1(s) \quad \ldots (22)$$

and $$C_2(s) = \frac{C_{in}(s)}{(\bar{t}_1.\bar{t}_2)(1+b)(s+P)(s+R)}$$

$$= C_{in}(s).H_2(s), \quad \ldots (23)$$

where $H_1(s), H_2(s)$ = transfer functions of V_1 and V_2 respectively,

$P = (F+G)/(2.\bar{t}_1.\bar{t}_2)$,

$R = (F-G)/(2.\bar{t}_1.\bar{t}_2)$,

$F = \bar{t}_1+\bar{t}_2$

and $G = [F^2 - (4.\bar{t}_1.\bar{t}_2)/(1+b)]^{1/2}$

Analogous to equation (12), it can be shown that

$$C_{in}(s) = C_o.(V_1+V_2)/Q$$

$$= C_o.(\bar{t}_1+\bar{t}_2)/(1+b).$$

where C_o refers to the mean concentration in V_1 and V_2. The inverse transform of equation (22) then becomes

$$C_1(t) = \frac{C_o.(\bar{t}_1+\bar{t}_2)}{(\bar{t}_1.\bar{t}_2)(P-R)}(P.\bar{t}_2-1).e^{-Pt} - (R.\bar{t}_2-1).e^{-Rt} \quad \ldots (24)$$

The mean residence time, $\bar{t}_A$, of the first tank can now be found by applying equation (7):

$$\bar{t}_A = (\bar{t}_1+\bar{t}_2)(1+b) - \bar{t}_2$$

It should be noted that $\bar{t}_A$ is related to the net flow rate, Q, and $\bar{t}_1$ to a flow rate of Q(1+b); hence the difference.

Equation (17) was solved for C_o, $\bar{t}_1$, $\bar{t}_2$ and b by fitting it to the data collected at point A, and $\bar{t}_A$ could be calculated. The fit is shown in Figure 17.

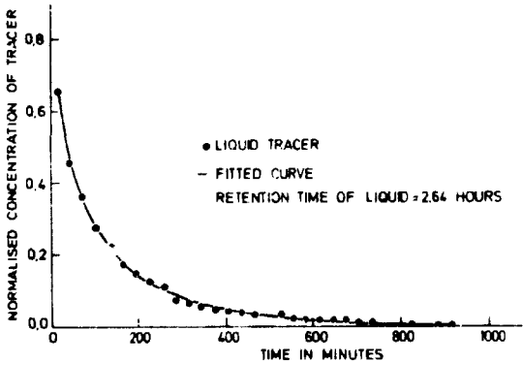

FIG.17 RESPONSE AT POINT (A) IN FIGURE 16

The second section of the plant consisted of five tanks in series, in parallel with two tanks in series. The tanks were of equal volume, V_3. The fraction of flow passing through each branch was unknown and could not be measured.

Let $C_{3a}(t)$ and $C_{3b}(t)$ be the response functions of the five tanks and two tanks respectively, and f the fraction of flow passing through the five tanks. If $C_3(t)$ is the response of the section, it follows that

$$C_3(t).Q = f.Q.C_{3a}(t) + (1-f).Q.C_{3b}(t)$$

or $$C_3(s) = f.C_{3a}(s) + (1-f).C_{3b}(s)$$

Applying equation (3),

$$C_3(s) = C_2(s).[f.H_{3a}(s) + (1-f).H_{3b}(s)]$$
$$= C_2(s).H_3(s) \quad \ldots (25)$$

where $H_{3a}(s)$ and $H_{3b}(s)$ are given by equation (19) as

$$H_{3a}(s) = 1/[(s.V_3/fQ) + 1]^5$$

$$H_{3b}(s) = 1/[(s.V_3/(1-f)Q) + 1]^2$$

and $H_3(s)$ = transfer function of the second section

$$= f.H_{3a}(s) + (1-f).H_{3b}(s)$$

The response of the last section's seven tanks, also of volume V_3, can be represented by

$$C_4(s) = C_3(s).H_4(s) \quad \ldots (26)$$

where $H_4(s) = 1/[(s.V_3/Q) + 1]^7$

Combining equations (23), (25) and (26),

$$C_4(s) = C_{in}(s).H_3(s).H_4(s) \quad \ldots (27)$$

In this case, $C_{in}(s)$ is defined as

$$C_{in}(s) = C_o.(\text{Total Volume})/Q$$
$$= C_o.(V_1+V_2+14V_3)/Q$$
$$= C_o.(\bar{t}_1+\bar{t}_2)(1+b) + 14.C_o.V_3/Q,$$

so that C_o refers to the mean concentration in all the tanks.

The inverse transform of $C_4(s)$ was not attempted, but by incorporating a numerical inversion method [5, 6] in a least-squares program [20], equation (27) could be solved for the remaining parameters V_3, f and C_o. The fit is shown in Figure 18.

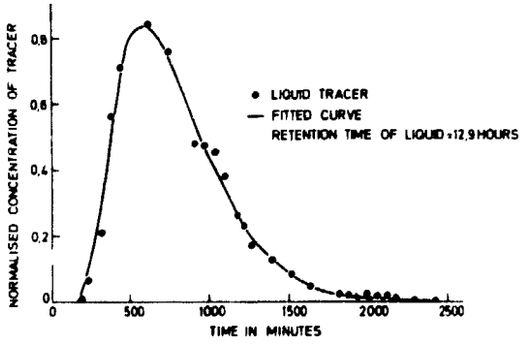

FIG.18 RESPONSE AT POINT (B) IN FIGURE 16

The usefulness of the modelling technique is reflected in this experiment in the evaluations of the recycle loop and the parallel flow of the second section. The measurement of flow fractions f and b was practically impossible in these particular plant conditions, so that a complete evaluation would not have been possible without the aid of the model.

5.2 Evaluation of Multiple Mixing Zones

The examples dealt with in 5.1 were concerned with plant conditions which were such that vessels could be represented as single mixing zones. This was possible mainly because of the high degree of mixing attained in the plants. Consequently, the models bore a physical resemblance to the plants. This should also be the aim

when multiple mixing zones in vessels with relatively poor mixing are modelled. The ideal model should not only simulate the response, but should be logically composed of models which identify possible mixing zones that can be visualized in the actual process.

This type of descriptive model has the advantage that predictions on plant behaviour can be made with better accuracy. In the field of chemical reaction kinetics, for instance, modelling has become a basic tool in the design of reaction vessels [7].

5.2.1 STAGNANCY

In the discussion so far, dead-volume zones and perfectly mixed zones have been defined. It is imaginable that as mixing becomes progressively poorer, some of the material will be less mixed than the rest. This type of behaviour is termed stagnancy. The formation of stagnant zones depends to a large extent on the shape of the vessel and the physical properties of the material. Stagnancy can be identified as a long 'tail' in the response. (Compare with the boundary-layer effect described in 3.2.) This signifies that some of the material is effectively retarded in the vessel.

This behaviour was encountered during an experiment at the gold leaching plant of the East Driefontein Gold Mine [22]. The plant was similar to that described in 5.1.1 (Figure 13). The effect was accompanied by dead volumes in excess of 40 %. Bearing this in mind, the possible flow pattern in a tank could be imagined as shown in Figure 19. Two zones of good mixing, with crossflow between zones, can be identified in this Figure. Figure 20 shows the model that is suggested by this pattern. The net flow of material through the lower zone is represented by bQ.

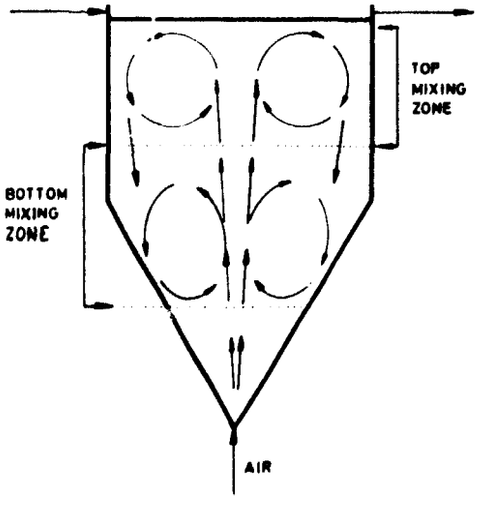

FIG 19 POSSIBLE FLOW PATTERN IN LEACHING TANK

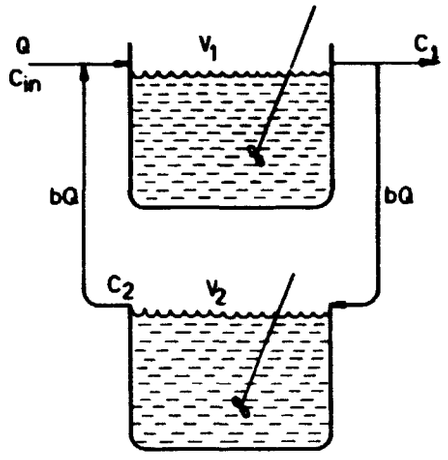

FIG 20 MODEL SUGGESTED BY FLOW PATTERN IN FIGURE 19

A comparison between this model and that of the first section of Figure 16 shows that equation (22) applies, with the following exceptions:

$$\bar{\tau}_1 = V_1/[Q.(1+b)],$$

$$\bar{\tau}_2 = V_2/(b.Q),$$

and $$C_{in}(s) = C_o.(V_1 + V_2)/Q$$

$$= C_o.[\bar{\tau}_1.(1+b) + \bar{\tau}_2.b]$$

In the general case of j such tanks in series, assuming that V_1, V_2 and b are the same for all the tanks, it can be shown that:

$$C_j(s) = C_o.[\bar{\tau}_1.(1+b) + \bar{\tau}_2.b].j.[H_1(s)]^j \qquad .. (28)$$

The fit of this equation to the response data of two tanks (j = 2) is shown in Figure 21. This is clearly an improvement on the tanks-in-series model (also shown in the Figure).

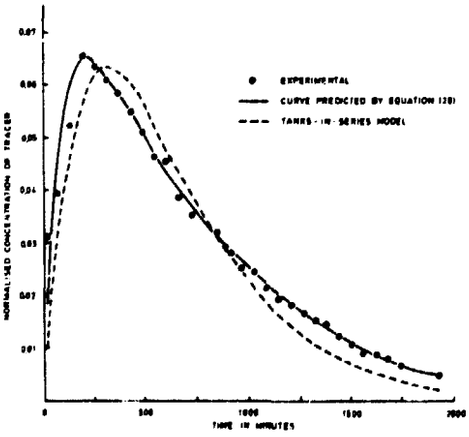

FIG 21 COMPARISON BETWEEN DIFFERENT MODELS APPLIED TO THE RESPONSE OF TWO TANKS

The assumption that $\bar{\tau}_1$, $\bar{\tau}_2$ and b are the same for all tanks is, strictly speaking, not valid. However, the model is simplified by such an assumption, and tracer data are in any case rarely accurate enough to justify such detailed modelling.

5.2.2 COMBINED MODELS

A very interesting model could be derived to describe the behaviour of potassium in a blast-furnace at ISCOR's Pretoria plant.

Irregularities in material balances of the natural potassium led to the suspicion that potassium was either *being temporarily retarded or accumulated* in the furnace. In an attempt to clarify this, ^{42}K was introduced in the form of K_2CO_3 into the furnace. Because of the powdery form of the tracer, it was sealed in four brass capsules in lead containers to prevent possible loss through the stack of the furnace. In this way, the capsules had to travel to a temperature region of 900 - 1 000 °C before the tracer was released. Samples of the slag output were taken at regular time intervals and the specific activity of each determined. Appropiate corrections for background and decay were made. The response is shown in Figure 22.

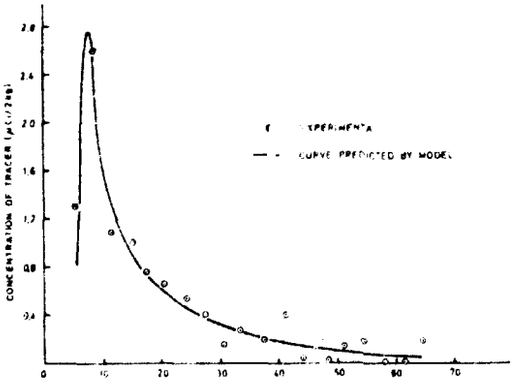

FIG 22 RESPONSE OF A BLAST FURNACE TO POTASSIUM TRACER

The initial time lag in the response was caused by the delay before the tracer was released. This can be represented by a plug-flow model of residence time $\bar{\tau}_1$, the response of which is $\delta(t-\bar{\tau}_1)$. This expresses a displacement of magnitude $\bar{\tau}_1$ of a unit delta function $\delta(t)$ along the time axis.

The initial distribution of the tracer in the furnace, after it had been released, may be represented by a perfectly mixed tank of residence time $\bar{\tau}_2$, and the mixing in the molten zone by a further mixed tank, $\bar{\tau}_3$. This combination still does not explain the long 'tail' of the response, which indicates the presence of some form of stagnancy. This can be included in the model as a recycle loop through a further mixed tank $\bar{\tau}_4$. The situation can be imagined physically if it is assumed that potassium compounds decomposed and vaporized in the molten zone to recondense on the walls and ore above. The downward movement of the ore would then reintroduce potassium into the active zone to complete the cycle.

The final model is shown in Figure 23. It can be shown that the response is

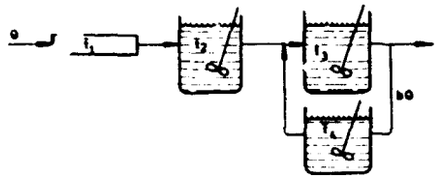

FIG 23 MODEL TO SIMULATE THE RESPONSE OF A BLAST FURNACE

$$C(s) = \frac{C_{in}(s).(s.\bar{\tau}_4 + 1)}{(s.\bar{\tau}_2+1).(1+b).(\bar{\tau}_3-\bar{\tau}_4).(s+P).(s+R)},$$

where P, R and b have the same meaning as previously. Since a delta function had in effect been injected at $t = \bar{\tau}_1$,

$$C_{in}(s) = C_o.(\text{Total Volume}/Q).L[S(t-\bar{\tau}_1)]$$
$$= C_o.[\bar{\tau}_1+\bar{\tau}_2+\bar{\tau}_3.(1+b)+\bar{\tau}_4.b].e^{-s\bar{\tau}_1}$$

The function could then be fitted to the data by the same method as in 5.1.2. The fit is shown in Figure 22.

Potassium accumulation in blast furnaces is not an unknown phenomenon. Although the scatter of data indicated that the potassium output was irregular, the mechanism according to which it occurred may have been that suggested by the model.

5.3 Simulation of Response

It is not always possible to construct a physically meaningful model for a particular process. The flow patterns may be so complex that the characteristics of individual flow regions cannot be identified in the response. Processes of this nature are often best analyzed by pure simulation of the response. The tanks-in-series model is easily adaptable for this purpose because, as it is, equation (16) expresses the response of any degree of mixing between no mixing (large j) and perfect mixing (j = 1). The application of the equation can be further extended by the use of the Stirling series:

$$(j-1)! = e^{-j}.j^{j-\frac{1}{2}}.(2\pi)^{\frac{1}{2}}.$$
$$(1 + 1/12j + 1/288j^2 - 139/51840j^3 - 571/2488320j^4 + \ldots.)$$

This approximation allows one to calculate the factorial for any real value of j, and not only integers.

The occasion to apply this principle arose when an attempt was made to evaluate the mixing in flotation cells used for the recovery of platinum-group metals at a

platinum mine [23]. The cells were square in shape and were contained in units of four cells. The divisions between cells in a unit were such that slurry could flow from one cell to the next through the entire depth of the cell. The aerating mechanisms were situated in the centres of the cells, near the bottom. It was required to determine the residence times of different size fractions of the solids in a unit of four cells.

The tracer was prepared by activating 250 g of each of the size fractions in the reactor to produce 10 mCi of ^{64}Cu and ^{24}Na as the main radioactive constituents. Because of the short residence time (± 3 min), on-stream measurements of the response were obtained by immersing a 25 mm sodium iodide detector in the outlet stream. The observed count rate was integrated over short periods and printed out on a printer. The response of the −53 μm fraction is shown in Figure 24.

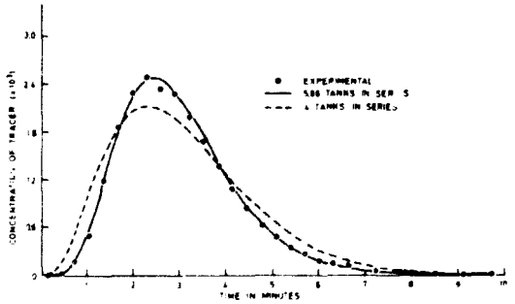

FIG. 24 RESPONSE OF FOUR FLOTATION CELLS

An attempt to fit four tanks in series (Figure 24) indicated that more tanks would be required to simulate the response. This could be explained only if the information of more than one mixing zone in a cell was postulated. The square-cell construction and the centrifugal forces created by the rotating aerating mechanism could have caused this.

Since the actual flow patterns could not be determined from the available data, it was decided to fit the tanks-in-series model (with a variable number of tanks) to the response. The fit is shown in Figure 24. This curve represents the behaviour of 5,86 perfectly mixed tanks, with a total residence time of 2,94 min. The number of tanks is a measure of the degree of mixing and has no other physical significance in this case.

A parallel-flow model, based on the same principles, can be easily constructed as a general model to simulate more complex flow patterns [18].

6. CONCLUSIONS

Tracer experimentation is possibly the most convenient tool for determining flow characteristics in industrial processes. The use of radioisotopes has in many cases the added advantage that the process material can be labelled, without any change in its physical and chemical properties. The fact that a radioactive tracer can be detected through the walls of a vessel is also an advantage when sampling would disturb the flow patterns, or when representative sampling may be difficult.

In conjunction with mathematical modelling, tracer measurements can be of immense value in the evaluation of the process and process economics, in that both quantitative and qualitative information about the process can be obtained.

By using the two basic models and techniques described in this report, many processes, ranging from gold recovery plants to sugar crystallizers, have been simulated to various degrees of accuracy. In some cases the results revealed information that could not have been obtained in any other way, such as deviations from the expected flow patterns. In other cases the models helped to confirm the faulty operation of equipment.

The construction of realistic models is usually based on possible physical occurrences that could have caused the experimentally observed response. In this respect care should be taken not to oversimplify a process or to attach so much significance to the model that the limitations set by the initial assumptions are exceeded.

7. REFERENCES

[1] Basson, J.K.; Snyman, G.C. Recent applications of isotope techniques. *S. Afr. Mech. Eng.* (1969) v. 18(11) p. 283 – 290.

[2] Exall, D.I. The study of mineral ores in grinding circuits with radiotracers. National conference on the technological applications of nuclear techniques, Pretoria, 1971. S. Afr. Atomic Energy Board, 1972, paper 21.

[3] Exall, D.I.; Taute, W.J. The distribution of activity in the batch milling of gold ore activated in a nuclear reactor. PEL-229. Apr 1973. 14 p. ISBN 0 86960 428 7.

[4] Erdélyi, A. Tables of integral transforms, Vol. 1. Mc Graw-Hill Book Company, New York, 1954.

[5] Stehfest, H. Numerical Inversion of Laplace transforms. Algorithm 368, Collected algorithms from CACM.

[6] Stroud, A.H.; Secrest, D. Gaussian Quadrature Formulas. Prentice-Hall Inc., Englewood Cliffs, N.J., 1966.

[7] Levenspiel, O. Chemical Reaction Engineering. John Wiley and Sons, London, 1966.

[8] Woodburn, E.T. A study of gas-phase axial mixing in a packed absorbtion tower. Thesis (Ph. D.), University of Witwatersrand, 1972. 255 p.

[9] Woodburn, E.T. The use of radio-isotopes in investigating the flow patterns in an industrial absorbtion tower. National conference on the

technological application of nuclear techniques, S. Afr. Atomic Energy Board, 1972, paper 9, p. 1 – 14.

[10] Snyman, G.C.; Short, R.C.; Basson, J.K. Air-flow measurements on the ventilation system of Kinross Gold Mine using radioactive krypton-85. Pin-153(BR). Dec 1972. 14 p. ISBN 0 86960 410 4.

[11] Taylor, G.I. The dispersion of matter in turbulent flow through a pipe. *Proc. Roy. Soc.* (1954) A233, 446 p. 446 – 468.

[12] Clayton, C.G. The measurement of flow of liquids and gases using radioactive isotopes. *J. Brit. Nucl. Energy Soc.* (Oct 1964) p. 252 – 268.

[13] Korbel, K. The shortest test length in the measurement of fluid flow velocity in a conduit by means of pulsed radioactive tracer injection. CSIR translation REF1031 from Inst. Nucl. Ph., Cracow, Report 764/PL, 1971.

[14] Hull, D.E. The total-count technique: A new principle of flow measurement. *Int. J. of Appl. Rad. and Isotopes* (1958) Vol. 4. p. 1 – 15.

[15] Snyman, G.C.; Short, R.C. Die gebruik van argon-41 om die volumetriese vloei van gas in 'n pyplyn te meet. Restricted report to South African Gas Distribution Corporation Ltd. PIN-155 (BR). Dec 1972. 8 p. ISBN 0 86960 412 0.

[16] Short, R.C.; Smith, S.W.; Snyman, G.C. Investigation of gas flow through a catalytic reactor at NATREF using radioactive argon-41 tracer. Restricted report to NATREF National Petroleum Refiners of South Africa (Pty) Ltd. PIN-221 (BR). Feb 1974. 12 p. ISBN 0 86960 492 9.

[17] Smith, S.W.; Short, R.C.; Snyman, G.C. The performance of continuous massecuite crystallizers investigated by iodine-131. Restricted report to Huletts Sugar Ltd. PIN-217 (BR). Mar 1974. 15 p. ISBN 0 86960 488 0.

[18] Himmelblau, D.M.; Bischoff, K.B. Process Analysis and Simulation: Deterministic Systems. John Wiley and Sons, New York, 1967.

[19] Snyman, G.C.; Short, R.C.; Smith, S.W. Retention times of solids and liquid in the Brown tanks of Libanon Gold Mining Company. Restricted report to Gold Fields of South Africa Ltd. PIN-196 (BR). Sep 1973. 11 p. ISBN 0 86960 461 9.

[20] Marquardt, D.W. An algorithm for least-squares estimation of nonlinear parameters. *J. Soc. Ind. Appl. Math.* (1963) v. 11(2) p. 431 – 441.

[21] Snyman, G.C.; Short, R.C.; Smith, S.W. Radioactive tracer measurement of the retention times of solids and liquid in the Brown tanks at Vaal Reefs North. Restricted report to Vaal Reefs Exploration and Mining Co. Ltd. PIN-203 (BR). Sep 1973. 19 p. ISBN 0 86960 474 0.

[22] Snyman, G.C.; Smith, S.W.; Short, R.C. Radioactive tracer measurement of the retention times of solids and liquid in the leaching Pachucas at East Driefontein Gold Mine. Restricted report to Gold Fields of South Africa Ltd. PIN-218 (BR). Feb 1974. 17 p. ISBN 0 86960 489 9.

[23] Smith, S.W.; Short, R.C.; Snyman, G.C. Residence-time measurement on flotation cells using radioactive platinum ore. Restricted report. PIN-237 (BR) Aug 1974. 22 p. ISBN 0 86960 514 3.

ISBN 0 86960 604 2